C. R. Mecanique 347 (2019) 463–476

Contents lists available at ScienceDirect

Comptes Rendus Mecanique

www.sciencedirect.com

A new analytical formula to compute the step length of Padé approximants in the ANM: Application to buckling structures

Rachida Ayane, Abdellah Hamdaoui, Bouazza Braikat *, Noureddine Tounsi, Noureddine Damil

Laboratoire d'ingénierie et matériaux (LIMAT), Faculté des sciences Ben M'Sik, Hassan II University of Casablanca, BP 7955, Sidi Othman, Casablanca, Morocco

ARTICLE INFO

Article history:
Received 5 May 2018
Accepted 24 April 2019
Available online 16 May 2019

Keywords:
Asymptotic Numerical Method (ANM)
Padé approximant
Buckling
Shells
Validity range
Step length

ABSTRACT

In this paper, we propose a new analytical formula to define the next branch in the Asymptotic Numerical Method (ANM) using the Padé approximants. The proposed formula is based on the computation of the relative error of two consecutive Padé approximants. This formula is obtained by developing the relative error with respect to the path parameter. An appropriate matrix formulation is adopted for the computation of this relative error. A comparison between the analytical formula proposed in this paper and the classical continuation Padé approximants using the step length computed numerically using dichotomy method is presented for examples of buckling structures.

1. Introduction

The analysis of physical phenomena has always required the resolution of systems of nonlinear equations. The most powerful numerical algorithm enabling us to solve these systems of equations is the Newton–Raphson one [1–3]. This method is based on two stages; a prediction and a correction. The principle of these strategies is to follow the branch in a stepwise manner via a succession of linearizations and some iterations to achieve the equilibrium. The complete solution is sought by a continuation type point by point. This method has been applied in many nonlinear problems of structures [2,4–8].

An alternative to this method is the Asymptotic Numeric Method (ANM), which is a continuation procedure that allows one to obtain the solution to nonlinear problems in a succession of analytical branches [9,10]. This method has been successfully applied in several works [11–18]. Each branch is determined by a representation in vectorial series over a validity range $[0, a^{s}_{max}]$ [10–12]. In these works, the step length a^{s}_{max} is computed by an explicit formula [10]. In order to increase this validity range, these vectorial series are often replaced by an appropriate vectorial Padé approximant [19–21].

The continuation Padé approximants is used for the first time by Elhage-Hussein et al. in [13]. In this work, the step length a^{p}_{max} is computed numerically by the dichotomy method. This computation of the step length a^{p}_{max} is based on the relative error $E_M(a)$ of two consecutive Padé approximants of order $M-1$, and M, respectively.

In this work, we propose for the first time to compute analytically the step length a^{p}_{max} of these Padé approximants by using a development with respect to the path parameter a of the relative error $E_M(a)$. This development is done by using

* Corresponding author.
E-mail addresses: b.braikat@gmail.com, bouazza.braikat@univh2c.ma (B. Braikat).

https://doi.org/10.1016/j.crme.2019.04.001
1631-0721/

an appropriate matrix formulation of the relative error. The smallest positive root of this polynomial corresponds to a good approximation of the step length $a^{\mathrm{p}}_{\max}$. In addition, we have made a comparison between the continuation Padé approximants used in the article [13] and the continuation Padé approximants proposed in this paper. The difference between these two continuations lies in the computation of the validity range $a^{\mathrm{p}}_{\max}$. In the continuation Padé approximants of paper [13], the validity range $a^{\mathrm{p}}_{\max}$ is numerically computed by the dichotomy method and, in the proposed continuation Padé approximants, it is given directly by the new explicit analytical formula. A comparison between this analytical formula and that used in [13] is made on examples of buckling structures.

This paper is organized as follows. In Section 2, the Asymptotic Numerical Method (ANM) and vectorial Padé approximants are presented. The proposition of an analytical formula of the step length $a^{\mathrm{p}}_{\max}$ is detailed in Section 3. In Section 4, two benchmarks are discussed in order to compare the continuation Padé approximants using the new analytical formula of the step length $a^{\mathrm{p}}_{\max}$ with the classical Padé approximant and series continuations. The first concerns the nonlinear bending of a plate and the second concerns the buckling of a cylindrical shell loaded in the center.

2. Asymptotic Numerical Method (ANM) and vectorial Padé approximant

Many engineering problems can be reduced to solve nonlinear problems depending on a control parameter λ. These problems are written in the following general form:

$$\{R(\{U\},\lambda)\} = \{0\} \tag{1}$$

where $\{U\}$ is the unknown vector of $\mathbb{R}^n$, λ is a parameter and $\{R\}$ is a vector function with values in $\mathbb{R}^n$ assumed to be sufficiently regular with respect to its arguments $\{U\}$, and λ. The Asymptotic Numerical Method (ANM) [16,22] is a family of algorithms for path-following problems. This principle is simply to expand the unknown $(\{U\},\lambda)$ of the nonlinear problem (1) in power series with respect to a path parameter a:

$$\begin{cases} \{U^s\}(a) - \{U^j\} &= \sum_{k=1}^{N} a^k \{U_k\} \\ \lambda^s(a) - \lambda^j &= \sum_{k=1}^{N} a^k \lambda_k \end{cases} \quad , \quad a \in [0, a^{\mathrm{s}}_{\max}] \tag{2}$$

where $(\{U^j\},\lambda^j)$ is a started vectorial solution, $(\{U_k\},\lambda_k)$ is a vectorial unknown and N is the truncation order of the series. The validity range $[0, a^{\mathrm{s}}_{\max}]$ is deduced from the computation of the truncated vector series (2). So, the step length $a^{\mathrm{s}}_{\max}$ is computed a posteriori by the following estimation, which has been proposed in [16]:

$$a^{\mathrm{s}}_{\max} = \left(\varepsilon_{\mathrm{s}} \frac{||\{U_1\}||}{||\{U_N\}||} \right)^{\frac{1}{N-1}} \tag{3}$$

where ε_{s} is a given tolerance parameter and $||.||$ indicates a standard norm. The step lengths depend on the definition of the path parameter a and we must add an auxiliary equation to define this parameter [16–18]. By using the evaluation of the series at $a = a^{\mathrm{s}}_{\max}$, we obtain a new starting point and define, in this way, the ANM continuation procedure. This continuation method has been proved to be an efficient method to compute the solution to nonlinear partial differential equations [9,11,12,16–18,22].

In order to increase the validity range of each solution branch, we replace the vectorial representation (2) by the vectorial Padé approximant of order $M = N - 1$:

$$\begin{cases} \{U^{\mathrm{p}}\}(a) - \{U^j\} &= \sum_{k=1}^{M} \dfrac{\Delta^M_{M-k}(a)}{\Delta^M_M(a)} a^k \{U_k\} \\ \lambda^{\mathrm{p}}(a) - \lambda^j &= \sum_{k=1}^{M} \dfrac{\Delta^M_{M-k}(a)}{\Delta^M_M(a)} a^k \lambda_k \end{cases} \quad , \quad a \in [0, a^{\mathrm{p}}_{\max}] \tag{4}$$

where $\Delta^M_k(a) = \sum_{i=0}^{k} b^M_i a^i$, $0 \le k \le M$, with b^M_0 is equal to 1, b^M_k, $1 \le k \le M$, are computed by a Gram–Schmidt orthonormalization technique of the vectors $\{U_k\}$, $1 \le k \le M$, and $a^{\mathrm{p}}_{\max}$ is a step length that determines the validity range of this approximant. Recall, for a given tolerance parameter ε_{p}, that the computation of the step length $a^{\mathrm{p}}_{\max}$ is done numerically by solving the following equation [13]:

$$\frac{||\{U^{\mathrm{p}}_M\}(a^{\mathrm{p}}_{\max}) - \{U^{\mathrm{p}}_{M-1}\}(a^{\mathrm{p}}_{\max})||_2}{||\{U^{\mathrm{p}}_M\}(a^{\mathrm{p}}_{\max}) - \{U^j\}||_2} - \varepsilon_{\mathrm{p}} = 0 \tag{5}$$

This Eq. (5) has been solved by the dichotomy method [16]. In the same way as in the case of the series continuation, we have proceed to a continuation of each branch by replacing $(\{U^j\},\lambda^j)$ by $\left(\{U\}(a^{\mathrm{p}}_{\max}),\lambda(a^{\mathrm{p}}_{\max})\right)$.

In order to facilitate the computation of the relative error $E_M(a)$, we propose, in this paper, to introduce a matrix formulation used recently in [23] of the rational representation (4) in the following form:

$$\{U^{\mathrm{p}}\}(a) - \{U^j\} \quad = \quad \frac{1}{\Delta_M^M(a)}[U_M][B_M]\{a_M\} \quad ; \quad a \in [0, a^{\mathrm{p}}_{\max}] \tag{6}$$

where $[U_M] = [\{U_1\} \cdots \{U_M\}]$ is the matrix of order $NDL \times M$ (NDL is the number of degrees of freedom) whose columns are the vectors $\{U_1\} \cdots \{U_M\}$, $[B_M]$ is the upper triangular matrix of order M defined by:

$$[B_M] = \begin{bmatrix} 1 & b_1^M & \cdots & b_{M-1}^M \\ \vdots & 1 & \cdots & \vdots \\ \vdots & & \ddots & b_1^M \\ 0 & \cdots & 0 & 1 \end{bmatrix} \tag{7}$$

and ${}^{\mathrm{t}}\{a_M\} = < a, a^2, \cdots, a^M >$.

The objective of the following section is to search analytically the step length $a^{\mathrm{p}}_{\max}$ by defining a relative error between two Padé approximants truncated at the consecutive orders $M-1$, and M.

3. Proposition of an analytical formula of the step length $a^{\mathrm{p}}_{\max}$

To establish an analytical formula of the step length $a^{\mathrm{p}}_{\max}$, let us recall that the relative error is given by:

$$E_M(a) = \frac{||\{U_M^p\}(a) - \{U_{M-1}^{\mathrm{p}}\}(a)||_2}{||\{U_M^{\mathrm{p}}\}(a) - \{U^j\}||_2} \tag{8}$$

With the help of the matrix formulation (6), it is shown that the formula (8) can be rewritten in the following form:

$$E_M(a) = a^{M-1} \frac{||\sum_{k=0}^{M-1} a^k [R_M]\{\varphi^k\}||_2}{||\sum_{k=0}^{2M-2} a^k [R_M]\{\eta^k\}||_2} \tag{9}$$

where $[R_M] = (\alpha_{ij})_{1 \le i \le j \le M}$ is an upper triangular square matrix of order M obtained by a factorization method $Q\,R$ from the matrix $[U_M]$; with α_{ij} are the orthogonalization coefficients of Gram–Schmidt, the vectors $\{\varphi^k\}$, $0 \le k \le M-1$, and $\{\eta^k\}$, $0 \le k \le 2M-2$ are functions of the coefficients b_k^M ($1 \le k \le M$) of the polynomial Δ_k^M of the Padé approximants truncated at orders M, and $M-1$, whose expressions are detailed in Appendix A.

By a simple computation (see Appendix B), we show that the development of the relative error $E_M(a)$ at order 3 with respect to the path parameter a in the neighborhood of 0 is written as:

$$E_M(a) = a^{M-1}(e_0 + e_1 a + e_2 a^2 + e_3 a^3 + O(a^4)) \tag{10}$$

where the computations of e_0, e_1, e_2, and e_3 are detailed in Appendix B. Taking into account Eqs. (5) and (10), the step length $a^{\mathrm{p}}_{\max}$ is solution to the following equation:

$$E_M(a) - \varepsilon_{\mathrm{p}} = 0 \tag{11}$$

The resolution of Eq. (11) consists in computing the roots of the polynomial $P(a)$ given by (see Appendix B):

$$P(a) = a^3 + \beta_2 a^2 + \beta_1 a + \beta_0 \tag{12}$$

where the coefficients β_0, β_1, and β_2 are given in Appendix B. In order to determine the roots of the polynomial $P(a)$, we replace the parameter a by $z - \dfrac{\beta_2}{3}$, which allows us to obtain the following equation verified by z:

$$z^3 + pz + q = 0 \tag{13}$$

where $p = \beta_1 - \dfrac{\beta_2^2}{3}$, and $q = \dfrac{2\beta_2^3}{27} - \dfrac{\beta_1\beta_2}{3} + \beta_0$. By introducing u, and v such that:

$$z = u + v, \tag{14}$$

Eq. (13) becomes:

$$u^3 + v^3 + (u+v)(3uv + p) + q = 0 \tag{15}$$

Therefore, if u, and v verify the following system

$$\begin{cases} u^3 + v^3 &= -q \\ uv &= -\dfrac{p}{3} \end{cases} \tag{16}$$

then u^3, and v^3 are the roots of the trinomial:

$$X^2 + qX - \frac{p^3}{27} = 0 \tag{17}$$

Then the roots of (17) for a positive discriminant $\Delta_0 = q^2 + 4\dfrac{p^3}{27} > 0$ are given by:

$$\begin{cases} u^3 &= \dfrac{-q + \sqrt{\Delta_0}}{2} \\ v^3 &= \dfrac{-q - \sqrt{\Delta_0}}{2} \end{cases} \tag{18}$$

Knowing the roots u, and v, then $z_1 = u + v$ is a root of (13). In the case where the discriminant is negative, there exists $\theta \in \mathbb{R}$ such that u^3, and v^3 verify

$$\begin{cases} u^3 &= \dfrac{-q + \mathrm{i}\sqrt{-\Delta_0}}{2} &= \sqrt{\dfrac{q^2 - \Delta_0}{4}}\exp^{\mathrm{i}\theta} \\ v^3 &= \dfrac{-q - \mathrm{i}\sqrt{-\Delta_0}}{2} &= \sqrt{\dfrac{q^2 - \Delta_0}{4}}\exp^{-\mathrm{i}\theta} \end{cases} \tag{19}$$

Therefore, $z_1 = \left(\dfrac{q^2 - \Delta_0}{4}\right)^{\frac{1}{6}} \left[\exp\left(\frac{\mathrm{i}\theta}{3}\right) + \exp\left(\frac{-\mathrm{i}\theta}{3}\right)\right] = 2\left(\dfrac{q^2 - \Delta_0}{4}\right)^{\frac{1}{6}} \cos\left(\dfrac{\theta}{3}\right)$ is a root of (13). Note that the equalities in (19) show that:

$$\theta = \arccos\left(\frac{-q}{\sqrt{q^2 - \Delta_0}}\right) \tag{20}$$

Knowing a root z_1 of (13), the other two roots z_2, and z_3 of (13) are those of the polynomial of degree 2 obtained by the Euclidean division of (13) by $z - z_1$. So, the roots of the polynomial $P(a)$ are given by:

$$\begin{cases} a_1 &= z_1 - \dfrac{\beta_2}{3} \\ a_2 &= z_2 - \dfrac{\beta_2}{3} \\ a_3 &= z_3 - \dfrac{\beta_2}{3} \end{cases} \tag{21}$$

Finally, the step length $a_{\max}^{\mathrm{p}}$ is given by the smallest positive root:

$$a_{\max}^{\mathrm{p}} = \min\left(a_1, a_2, a_3\right) \tag{22}$$

4. Numerical applications

In this section, we have computed analytically the smallest positive real root of (19) that we have compared with the value of $a_{\max}^{\mathrm{p}}$ obtained by the dichotomy method applied to Eq. (7) for the same residual. The used coefficients b_i^M of the Padé approximant are those computed by the Gram–Shmidt orthonormalization technique of the vectors $\{U_{\mathrm{i}}\}$ $(1 \leq i \leq M)$. A comparison between this new formula (19) and the one determined numerically by the dichotomy method is illustrated on examples of bending and buckling of structures. The $DKT18$ element is used for finite element analysis [24,25].

4.1. Nonlinear bending of a square plate

We consider the nonlinear bending of an elastic, homogeneous and isotropic square plate of length $L = 200$ mm and thickness $h = 1$ mm, embedded at the four edges and subjected to vertical loading λF in its center, with $F = 4$ N. The

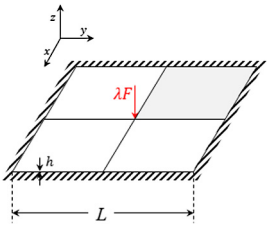

Fig. 1. Geometrical characteristics of the plate.

Table 1
Comparison between the results obtained by 8 ANM steps of the three types of continuation CS, CPC, and CPA for the order $N = 10$ and for the tolerance parameters $\varepsilon_s = 1{\cdot}10^{-7}$, $\varepsilon_p = 7.98{\cdot}10^{-5}$, and $\varepsilon_p = 1.5{\cdot}10^{-3}$, respectively.

Order	CS, $\varepsilon_s = 1.0{\cdot}10^{-7}$			CPC, $\varepsilon_p = 7.89{\cdot}10^{-5}$			CPA, $\varepsilon_p = 1.5{\cdot}10^{-3}$		
10	N (steps)	λ	w	N (steps)	λ	w	N (steps)	λ	w
	8	14.41	1.34	8	202.6	4.06	8	208.9	4.10

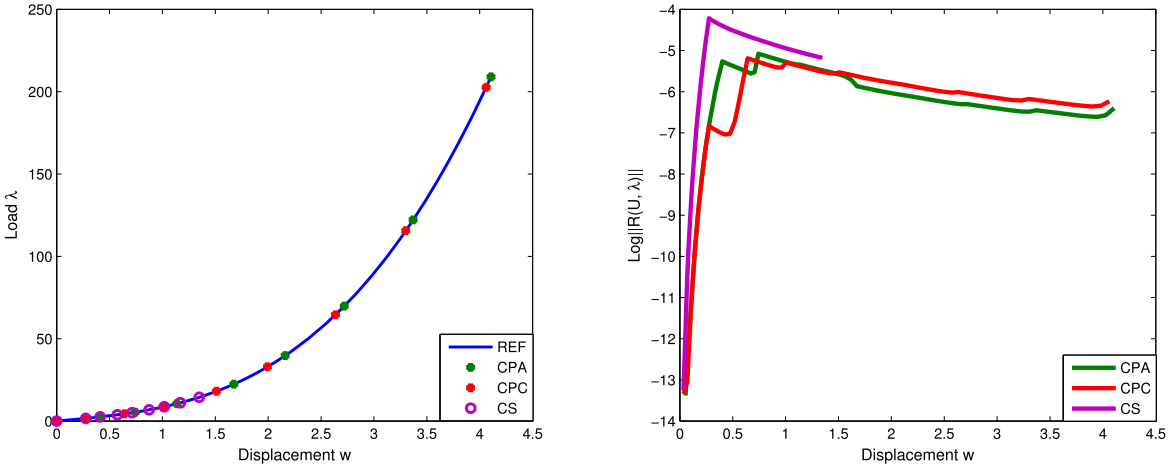

(a) Load-displacement curve (b) Residual-displacement curve

Fig. 2. Load-displacement and residual-displacement curves obtained by 8 ANM steps of the three algorithms CS, CPC, and CPA for the truncation order $N = 10$.

mechanical characteristics of this plate are: Young's modulus $E = 3{\cdot}10^4$ MPa and Poisson's ratio $\nu = 0.3$ (see Fig. 1). The plate is discretized in 32 $DKT18$ finite elements, i.e. 150 degrees of freedom.

In this numerical experiment, the obtained results are compared between three types of continuations. The first is a continuation series CS using the representation (2), the second is a continuation Padé approximant using the representation (4), where the step length a^p_{max} is computed by the dichotomy method CPC and the third is a continuation Padé approximant using the representation (4) where the step length a^p_{max} is defined by the analytical formula (19) CPA.

In Table 1, we report the results obtained by 8 ANM steps with the truncation orders $N = 10$ for the same residual. Note that with the continuation series CS, we have reached a deflection $w = 1.34$ mm, however with the continuation Padé of type CPC, we have reached a deflection $w = 4.06$ mm. If we use the continuation Padé of type CPA with the new formula of step length a^p_{max}, we have reached a deflection $w = 4.10$ mm. From the obtained results, we note that for $N = 10$, the proposed analytical formula works well and gives same results as the dichotomy method.

In Fig. 2, we present a comparison between the results obtained at the forced node by the continuation series CS and the continuation Padé approximant using the two definitions of the step length a^p_{max} CPC, and CPA. These results are obtained with the truncation order $N = 10$ in 8 ANM steps and with a tolerance parameter that gives the same quality of the solution (see Fig. 2b). From these results, we note that the two continuations of Padé approximants are comparable.

In Table 2, we show a comparison between the results obtained by the continuation series CS and the continuation Padé where the step length a^p_{max} is computed by the dichotomy method and by the proposed analytical formula (19). These results are obtained with a truncation order $N = 16$ in 8 ANM steps. According to this table, we note that, also for this

Table 2
Comparison between the results obtained by 8 ANM steps of the three types of continuation CS, CPC, and CPA for the order $N = 16$ and for the tolerance parameters $\varepsilon_s = 1.0{\cdot}10^{-7}$, $\varepsilon_p = 1.0{\cdot}10^{-4.2}$, and $\varepsilon_p = 1.1{\cdot}10^{-3}$, respectively.

Order	CS, $\varepsilon_s = 1.0{\cdot}10^{-7}$			CPC, $\varepsilon_p = 1.0{\cdot}10^{-4.2}$			CPA, $\varepsilon_p = 1.1{\cdot}10^{-3}$		
16	N (steps)	λ	w	N (steps)	λ	w	N (steps)	λ	w
	8	48.59	2.35	8	157.5	3.70	8	275.8	4.53

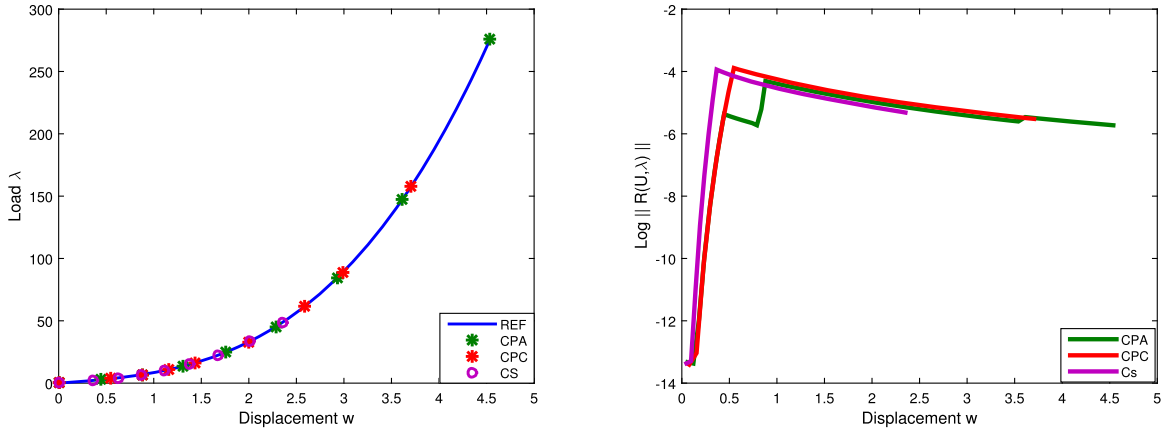

(a) Load-displacement curve (b) Residual-displacement curve

Fig. 3. Load-displacement and Residual-displacement curves obtained by 8 ANM steps of the three algorithms CS, CPC, and CPA for the truncation order $N = 16$.

Table 3
Comparison between the results obtained by 8 ANM steps of the three types of continuation CS, CPC, and CPA for the order $N = 20$ and for the tolerance parameters $\varepsilon_s = 10^{-7}$, $\varepsilon_p = 5{\cdot}10^{-5}$, and $\varepsilon_p = 3.211{\cdot}10^{-4}$, respectively.

Order	CS, $\varepsilon_s = 10^{-7}$			CPC, $\varepsilon_p = 5{\cdot}10^{-5}$			CPA, $\varepsilon_p = 3.211{\cdot}10^{-4}$		
20	N (steps)	λ	w	N (steps)	λ	w	N (steps)	λ	w
	8	76.08	2.81	8	178.2	3.87	8	272.9	4.52

choice of order $N = 16$, the continuation Padé approximant using the analytical formula (19) to compute the step length a^p_{max} gives good results. With 8 ANM steps, we reach a deflection of $w = 4.53$.

Fig. 3 illustrates the load-displacement and residual-displacement curves at the forced node obtained by 8 ANM steps of the three continuations CS, CPC, and CPA for the truncation order $N = 16$ and for the tolerance parameter that gives the same quality of solution.

Table 3 represents a comparison between the results obtained by the three continuations CS, CPC, and CPA for the truncation order $N = 20$ in 8 ANM steps and for tolerance parameters that give the same quality of solution. From the obtained results, it is clear that the step length of the continuation CPA are greater here than those of the two other continuations.

Fig. 4 illustrates the load-displacement and residual-displacement curves at the forced node obtained by 8 ANM steps of the three continuations CS, CPC, and CPA for the truncation order $N = 20$ and for the tolerance parameter that gives the same quality of solution.

4.2. Buckling of a cylindrical shell loaded in the center

This second application concerns the buckling of a cylindrical shell articulated along the two opposite edges and free on the two other ones. This structure is of length $2L = 504$ mm, of radius $R = 2540$ mm, and has an angle of half opening $\theta = 0.1$ rad, made of a homogeneous, elastic, and isotropic material of Young's modulus $E = 3102.75$ MPa and Poisson's coefficient $\nu = 0.3$, subjected to a vertical loading λF applied at its center, with $F = 1000$ N. Due to the symmetry, only a quarter of the structure is discretized in 200 triangular elements of type $DKT18$, i.e. 726 degrees of freedom. Two types of thickness are studied in this application: $h = 12.7$ mm and $h = 6.35$ mm (see Fig. 5). For this benchmark example, the response curve based on the value of the thickness h has limit points in λ, and w. This is a good test for the continuation methods [12,22].

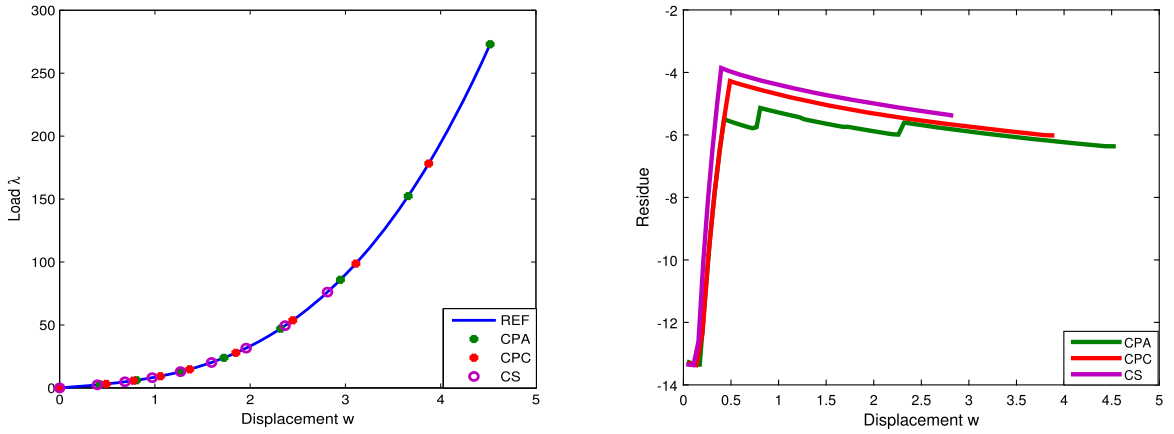

(a) Load-displacement curve (b) Residual-displacement curve

Fig. 4. Load-displacement and residual-displacement curves obtained by 8 ANM steps of the three algorithms CS, CPC, and CPA for the truncation order $N = 20$.

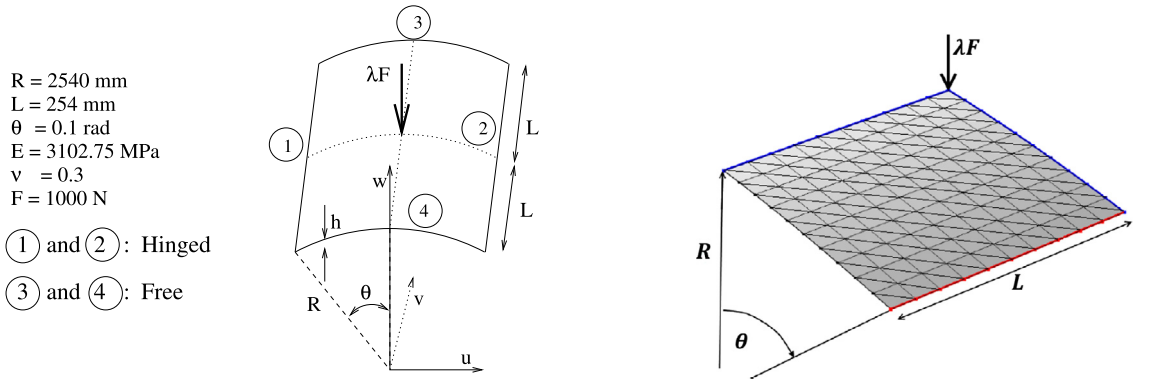

(a) Geometrical and mechanical characteristics (b) Used mesh

Fig. 5. Geometrical and mechanical characteristics of the studied structure and the used mesh.

Table 4
Comparison between the results obtained by 6 ANM steps of the three types of continuation CS, CPC, and CPA for the order $N = 10$ and for the tolerance parameters $\varepsilon_s = 3{\cdot}10^{-6}$, $\varepsilon_p = 10^{-6}$, and $\varepsilon_p = 1.7{\cdot}10^{-5.1}$, respectively.

Order	CS, $\varepsilon_s = 3{\cdot}10^{-6}$			CPC, $\varepsilon_p = 10^{-6}$			CPA, $\varepsilon_p = 1.7{\cdot}10^{-5.1}$		
10	N (steps)	λ	w	N (steps)	λ	w	N (steps)	λ	w
	6	0.75	22.01	6	0.78	22.2	6	1.27	24.4

In this second numerical experiment, we treat first the buckling of a thick cylindrical shell ($h = 12.7$ mm) while comparing the results obtained by the three types of continuations CS, CPC, and CPA. We made the same numerical study as in the first example.

In Table 4, we report the results obtained by 6 ANM steps with the truncation order $N = 10$ for the same residual. The parameters ε_s, and ε_p have been chosen in order to get the same residual. Note that with the continuation series CS, we have reached a deflection $w = 22.01$ mm, however with the continuation Padé approximant CPC, we have reached a deflection $w = 22.2$ mm. If we use the continuation Padé approximant CPA with the new proposed formula (19) of a^{p}_{max}, we have reached a deflection $w = 24.4$ mm. From the obtained results, we note that for $N = 10$, the proposed analytical formula is less better than the two other in this example.

In Fig. 6, we present a comparison between the results obtained at the forced node by the continuation series and the continuation Padé using the two definitions of the step length a^{p}_{max}. These results are obtained with the truncation order $N = 10$ in 6 ANM steps and with a tolerance parameter that gives the same quality of solution (see Fig. 6b).

Table 5 represents a comparison between the results obtained by the three continuations CS, CPC, and CPA for the truncation order $N = 15$ in 5 ANM steps and for the tolerance parameters ε_s, and ε_p that give the same quality of solution.

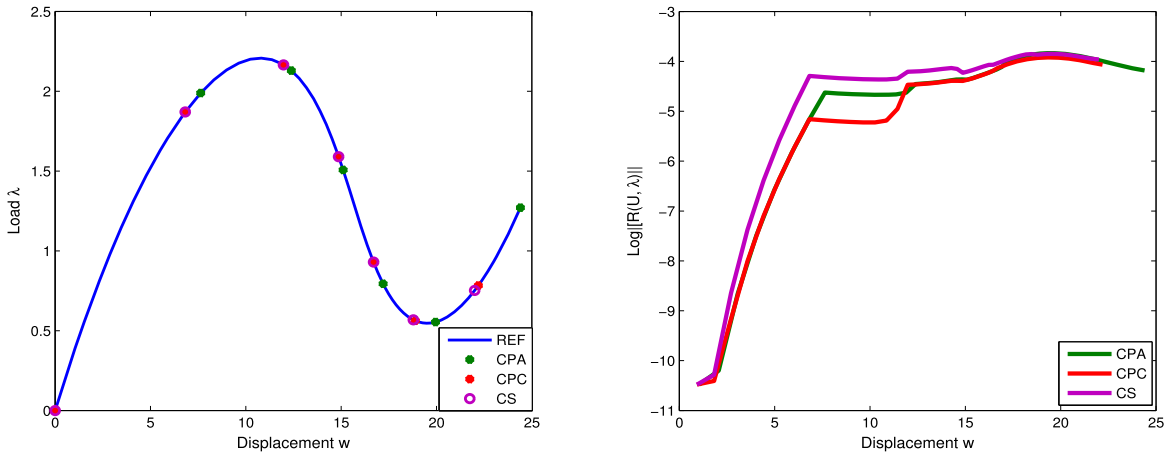

(a) Load-displacement curve (b) Residual-displacement curve

Fig. 6. Load-displacement and residual curves for $h = 12.7$ mm and $N = 10$ obtained by 6 ANM steps of the three continuations CS, CPC, and CPA.

Table 5
Comparison between the results obtained by 5 ANM steps of the three types of continuation CS, CPC, and CPA for the order $N = 15$ and for the tolerance parameters $\varepsilon_s = 2.0{\cdot}10^{-6}$, $\varepsilon_p = 10^{-6}$, and $\varepsilon_p = 8.0{\cdot}10^{-5}$, respectively.

Order	CS, $\varepsilon_s = 2.0{\cdot}10^{-6}$			CPC, $\varepsilon_p = 10^{-6}$			CPA, $\varepsilon_p = 8.0{\cdot}10^{-5}$		
15	N (steps)	λ	w	N (steps)	λ	w	N (steps)	λ	w
	5	2.47	27.8	5	17.38	44.44	5	28.53	51.03

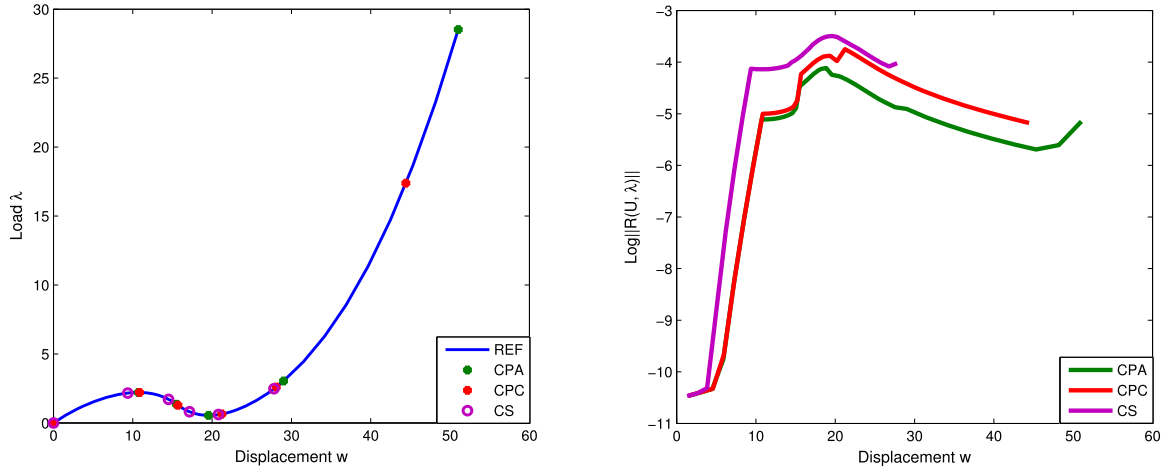

(a) Load-displacement curve (b) Residual-displacement curve

Fig. 7. Load-displacement and residual curves for $h = 12.7$ mm and $N = 15$ obtained by 5 ANM steps of the three continuations CS, CPC, and CPA.

From the obtained results, it is clear that the step length of the continuation Padé approximant CPA is greater here than those of the two other continuations.

In Fig. 7, we present a comparison between the results obtained at the forced node by the continuation series and the continuation Padé approximant using the two definitions of the step length a^p_{max}. These results are obtained with the truncation order $N = 15$ in 5 ANM steps and with a tolerance parameter that gives the same quality of solution (see Fig. 7b).

Table 6 provides a comparison between the results obtained by the three continuations CS, CPC, and CPA for the truncation order $N = 20$ in 4 ANM steps and for the tolerance parameters ε_s, and ε_p that give the same quality of solution. From the obtained results, it is clear that the step length of the continuation CPA is greater here than those of the two other continuations.

Table 6
Comparison between the results obtained by 4 ANM steps of the three types of continuation CS, CPC, and CPA for the order $N = 20$ and for the tolerance parameters $\varepsilon_s = 2.0{\cdot}10^{-6}$, $\varepsilon_p = 5.0{\cdot}10^{-6}$, and $\varepsilon_p = 10^{-4.1}$, respectively.

Order	CS, $\varepsilon_s = 2.0{\cdot}10^{-6}$			CPC, $\varepsilon_p = 5.0{\cdot}10^{-6}$			CPA, $\varepsilon_p = 10^{-4.1}$		
20	N (steps)	λ	w	N (steps)	λ	w	N (steps)	λ	w
	4	2.39	27.6	4	13.11	41.19	4	15.24	42.88

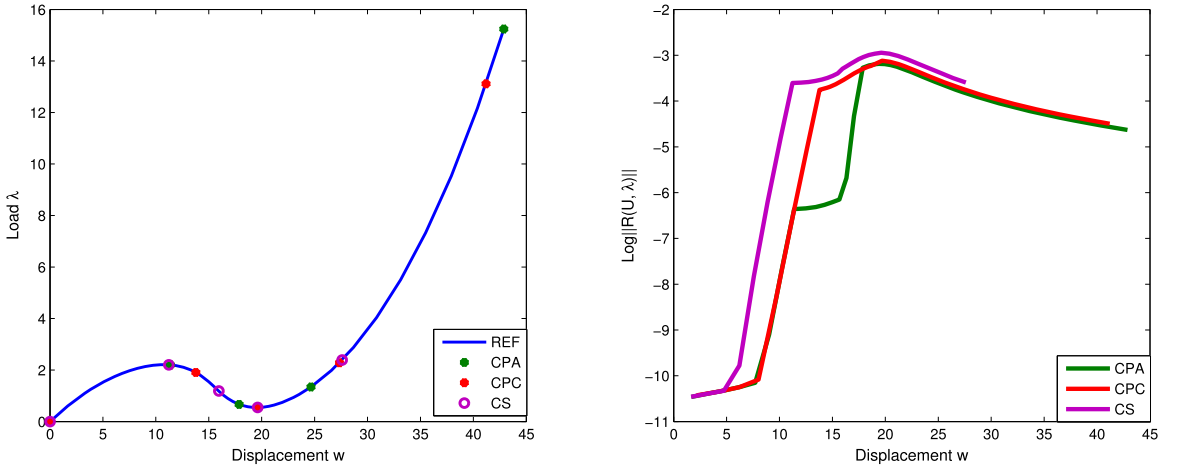

(a) Load-displacement curve (b) Residual-displacement curve

Fig. 8. Load-displacement and residual-displacement curves for $h = 12.7$ mm and $N = 20$ obtained by 4 ANM steps of the three continuations CS, CPC, and CPA.

Table 7
Comparison between the results obtained by 22 ANM steps of the three types of continuation CS, CPC, and CPA for the order $N = 10$ and for the tolerance parameters $\varepsilon_s = 6.0{\cdot}10^{-7}$, $\varepsilon_p = 12.0{\cdot}10^{-7}$, and $\varepsilon_p = 9.3{\cdot}10^{-6}$, respectively.

Order	CS, $\varepsilon_s = 6.0{\cdot}10^{-7}$			CPC, $\varepsilon_p = 12.0{\cdot}10^{-7}$			CPA, $\varepsilon_p = 9.3{\cdot}10^{-6}$		
10	N (steps)	λ	w	N (steps)	λ	w	N (steps)	λ	w
	22	−0.36	17.38	22	0.67	29.97	22	0.64	29.80

In Fig. 8, we present a comparison between the results obtained at the forced node by the continuation series and the continuation Padé approximant using the two definitions of the step length a^p_{max}. These results are obtained with the truncation order $N = 20$ in 4 ANM steps and with tolerance parameters ε_s, and ε_p that give the same quality of solution (see Fig. 8b).

In this second numerical experiment, we treat also the buckling of a thin cylindrical shell ($h = 6.35$ mm) while comparing the results obtained by the three continuations CS, CPC, and CPA.

In Table 7, we report the results obtained by 22 ANM steps with the truncation order $N = 10$ for the same residual. Note that with the continuation series CS, we have reached a deflection $w = 17.38$ mm, however with the continuation Padé approximant CPC, we have reached a deflection $w = 29.97$ mm. If we use the continuation Padé CPA with the new formula (19) of the step length a^p_{max}, we have reached a deflection $w = 29.80$ mm.

In Fig. 9, we present a comparison between the results obtained at the forced node by 22 ANM steps of the three continuations CS, CPC, and CPA with the truncation order $N = 10$ and with a tolerance parameter that gives the same quality of solution (see Fig. 9b).

Table 8 presents a comparison between the results obtained by 16 ANM steps of the three continuations CS, CPC, and CPA for the truncation order $N = 15$ and for the tolerance parameter that gives de same quality of solution. From the obtained results, it is clear that the step length of the continuation CPA is less here than those of the two other continuations.

In Fig. 10, we present a comparison between the results obtained at the forced node by 16 ANM steps of the three continuations CS, CPC, and CPA. These results are obtained with the truncation order $N = 15$ and with a tolerance parameter that gives the same quality of solution (see Fig. 10b).

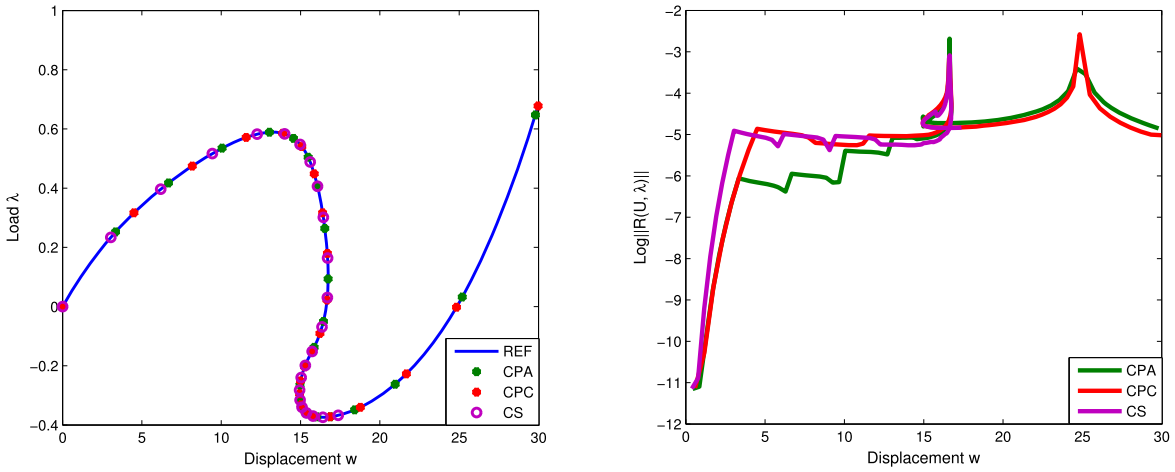

(a) Load-displacement curve (b) Residual-displacement curve

Fig. 9. Load-displacement and residual-displacement curves for $h = 6.35$ mm and $N = 10$ obtained by 22 ANM steps of the three continuations CS, CPC, and CPA.

Table 8
Comparison between the results obtained by 16 ANM steps of the three types of continuation CS, CPC, and CPA for the order $N = 15$ and for the tolerance parameters $\varepsilon_s = 6.0{\cdot}10^{-8}$, $\varepsilon_p = 6.0{\cdot}10^{-8}$, and $\varepsilon_p = 12.0{\cdot}10^{-7}$, respectively.

Order	CS, $\varepsilon_s = 6.0{\cdot}10^{-8}$			CPC, $\varepsilon_p = 6.0{\cdot}10^{-8}$			CPA, $\varepsilon_p = 12.0{\cdot}10^{-7}$		
15	N (steps)	λ	w	N (steps)	λ	w	N (steps)	λ	w
	16	−0.37	16.34	16	0.31	27.62	16	0.18	26.58

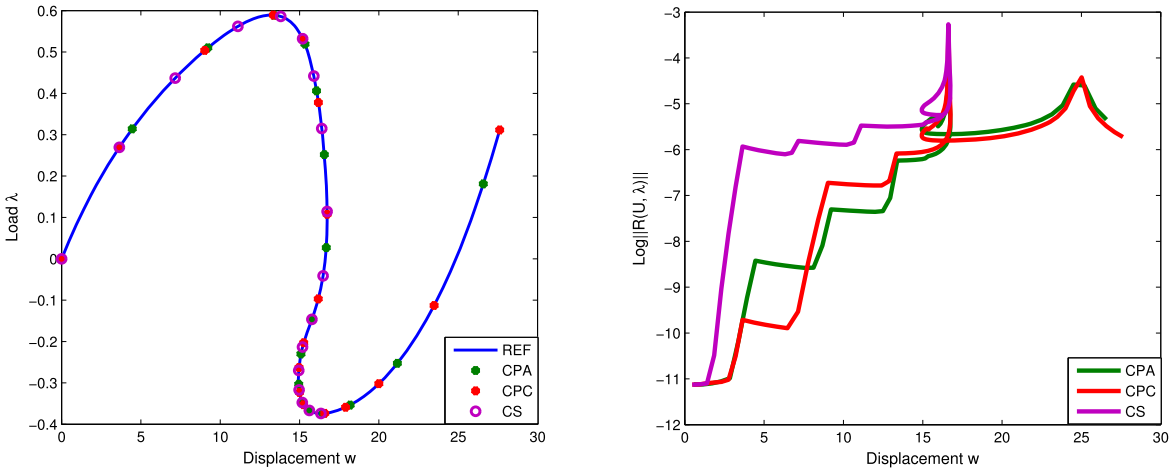

(a) Load-displacement curve (b) Residual-displacement curve

Fig. 10. Load-displacement and residual curves for $h = 6.35$ mm and $N = 15$ obtained by 16 ANM steps of the three continuations CS, CPC, and CPA.

Table 9 presents a comparison between the results obtained by 14 ANM steps of the three continuations CS, CPC, and CPA for the truncation order $N = 20$ and for the tolerance parameter that gives the same quality of solution. From the obtained results, it is clear that the step length of the continuation CPA is less here than those of the two other continuations.

In Fig. 11, we present a comparison between the results obtained at the forced node by 14 ANM steps of the three continuations CS, CPC, and CPA. These results are obtained with the truncation order $N = 20$ and with a tolerance parameter that gives the same quality of solution (see Fig. 11b).

Table 9
Comparison between the results obtained by 14 ANM steps of the three continuations CS, CPC, and CPA for the order $N = 20$ and for the tolerance parameters $\varepsilon_s = 10^{-8}$, $\varepsilon_p = 10^{-9.5}$, and $\varepsilon_p = 10^{-6.14}$, respectively.

Order	CS, $\varepsilon_s = 10^{-8}$			CPC, $\varepsilon_p = 10^{-9.5}$			CPA, $\varepsilon_p = 10^{-6.14}$		
20	N (steps)	λ	w	N (steps)	λ	w	N (steps)	λ	w
	14	−0.37	16.74	14	1.01	31.7	14	0.84	30.85

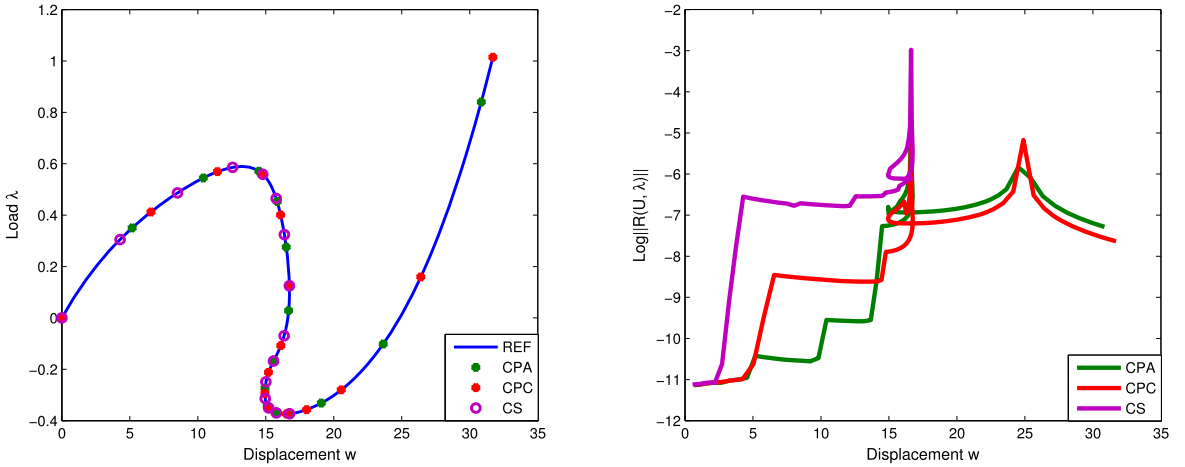

(a) Load-displacement curve (b) Residual-displacement curve

Fig. 11. Load-displacement and residual curves for $h = 6.35$ mm and $N = 20$ obtained by 14 ANM steps of the three continuations CS, CPC, and CPA.

It should be noted that the continuation CPC uses the numerical solution a^{p}_{max} to Eq. (5) when the pole of the denominator of the Padé approximants is greater than a^{s}_{max} of Eq. (3) and otherwise it uses a^{s}_{max}, whereas the continuation CPA always uses a^{p}_{max} of Eq. (22).

5. Conclusion

In this work, we have proposed an analytical formula of the step length a^{p}_{max} that defines the validity range of Padé approximants in the ANM algorithm. In order to determine this formula, we have defined the relative error between two consecutive vectorial Padé approximants. Then, with the help of a matrix formulation, we have developed this relative error at the order 3. From the obtained results, it can be seen that, when this new analytical formula, is used it is possible to ensure a purely Padé continuation. Moreover, it is clear that the proposed formula makes it possible to have comparable step lengths with the same residual compared to continuations of series CPS and Padé using the dichotomy method CPC. It should be noted also that the continuation CPC requires, in addition, the computation time of a^{p}_{max} from Eq. (5).

Appendix A. Computation of the vectors $\{\varphi^k\}$, and $\{\eta^k\}$

The components φ^k_i, $1 \le i \le M$ of vectors $\{\varphi^k\}$, $0 \le k \le M-1$ that appear in Eq. (9) are such that:

$$\varphi^0_i = \begin{cases} b^{M-1}_{M-i} & for \quad 1 \le i \le M-1 \\ 1 & for \quad i = M \end{cases}, \varphi^{M-1}_i = \begin{cases} b^{M-1}_{M-1} b^{M}_{M-i} - b^{M}_{M} b^{M-1}_{M-i-1} & for \quad 1 \le i \le M-1 \\ b^{M-1}_{M-1} & for \quad i = M \end{cases} \tag{23}$$

and, for $1 \le k \le M-2$,

$$\varphi^k_i = \begin{cases} b^{M-1}_{k} b^{M}_{M-i} + b^{M-1}_{M-1} b^{M}_{k-i+1} + \sum_{n=k+1}^{M-2} \left(b^{M-1}_{n} b^{M}_{M+k-i-n} - b^{M}_{n} b^{M-1}_{M+k-i-n} \right) & \\ -b^{M}_{M-1} b^{M-1}_{k-i+1} - b^{M}_{M} b^{M-1}_{k-i} & for \quad 1 \le i \le k, \\ b^{M-1}_{k} b^{M}_{M-i} + \sum_{n=k+1}^{M+k-i} \left(b^{M-1}_{n} b^{M}_{M+k-i-n} - b^{M}_{n} b^{M-1}_{M+k-i-n} \right) & for \quad k+1 \le i \le M-1 \\ b^{M-1}_{k} & for \quad i = M \end{cases} \tag{24}$$

The other vectors $\{\eta^k\}$ for $0 \le k \le 2M-2$ are given by:

$$\{\eta^k\} = \begin{cases} {}^{\mathrm{t}} < 1, 0, \cdots, 0 > & for \quad k = 0 \\ {}^{\mathrm{t}} < f_k, f_{k-1}, \cdots, f_1, 1, 0, \cdots, 0 > & for \quad 1 \le k \le M-1 \\ {}^{\mathrm{t}} < g^M_{1,k-M}, g^M_{2,k-M}, \cdots, g^M_{M,k-M} > & for \quad M \le k \le 2M-1 \end{cases} \tag{25}$$

where the components f_k, and $g^M_{i,k-M}$ are given by:

$$\begin{cases} f_k &= \sum_{n=0}^{k} b_n^M b_{k-n}^{M-1} & for \quad 1 \le k \le M-1 \\ g^M_{i,k} &= \sum_{n=k}^{Min(M-1;M+k-\mathrm{i})} b_n^{M-1} b^M_{M+k-i-n} & for \quad 1 \le \mathrm{i} \le M, \quad 1 \le k \le M-1 \end{cases} \tag{26}$$

as explained in the paper [23].

Appendix B. Computation of the polynomial $P(a)$

In order to approach $E_M(a) - \varepsilon_{\mathrm{p}}$ of Eq. (11) by its truncated development at the order 3 with respect to the parameter a in the neighborhood of 0, let

$$\begin{aligned} \{\gamma^k\} &= [R_M]\{\varphi^k\} \quad for \quad 0 \le k \le M-1 \\ \{\xi^k\} &= [R_M]\{\eta^k\} \quad for \quad 0 \le k \le 2M-2 \end{aligned} \tag{27}$$

We have

$$E_M^2(a) = a^{2M-2} \frac{H(a)}{Q(a)} \tag{28}$$

where $H(a)$, and $Q(a)$ are given by:

$$\begin{cases} H(a) &= ||\{\gamma^0\}||_2^2 + (2 < \gamma^0 > \{\gamma^1\})a + (< \gamma^0 > \{\gamma^2\} + ||\{\gamma^1\}||_2^2)a^2 + 2(< \gamma^1 > \{\gamma^2\} + < \gamma^0 > \{\gamma^3\})a^3 \\ & \quad + O(a^4) \\ Q(a) &= ||\xi^0||_2^2 + (2 < \xi^0 > \{\xi^1\})a + (< \xi^0 > \{\xi^2\} + ||\xi^1||_2^2)a^2 + 2(< \xi^1 > \{\xi^2\} + < \xi^0 > \{\xi^3\})a^3 + O(a^4) \end{cases} \tag{29}$$

Subsequently, for a small enough, we have:

$$E_M(a) = a^{M-1}\left(e_0 + e_1 a + e_2 a^2 + e_3 a^3 + O(a^4)\right) \tag{30}$$

where e_0, e_1, e_2, and e_3 are given by:

$$\begin{cases} e_0 &= \left(\dfrac{\|\{\gamma^0\}\|_2^2}{||\{\xi^0\}||_2^2}\right)^{\frac{1}{2}} \\ e_1 &= \dfrac{e_0}{2} B \\ e_2 &= e_0\left(\dfrac{G}{2} - \dfrac{B^2}{8}\right) \\ e_3 &= \dfrac{e_0 H}{2} - \dfrac{e_0 B G}{4} + \dfrac{e_0 H^3}{16} \end{cases} \tag{31}$$

with

$$\begin{cases} B = \dfrac{2 < \gamma^0 > \{\gamma^1\}}{\|\{\gamma^0\}\|_2^2} - \dfrac{2 < \xi^0 > \{\xi^1\}}{\|\{\xi^0\}\|_2^2} \\ C = \left(\dfrac{2 < \xi^0 > \{\xi^1\}}{\|\{\xi^0\}\|_2^2}\right)^2 - \dfrac{2 < \xi^0 > \{\xi^2\} + \|\{\xi^1\}\|_2^2}{\|\{\xi^0\}\|_2^2} \\ D = -4\dfrac{< \xi^0 > \{\xi^1\} < \gamma^0 > \{\gamma^1\}}{\|\{\xi^0\}\|_2^2} \\ E = 2 < \gamma^0 > \{\gamma^2\} + \|\{\gamma^1\}\|_2^2 \\ F = \|\{\gamma^0\}\|_2^2 \left(4\dfrac{< \xi^0 > \{\xi^1\}}{\|\{\xi^0\}\|_2^2}\dfrac{\left(2 < \xi^0 > \{\xi^2\} + \|\{\xi^1\}\|_2^2\right)}{\|\{\xi^0\}\|_2^2} - 8\left(\dfrac{< \xi^0 > \{\xi^1\}}{\|\{\xi^0\}\|_2^2}\right)^3 - 2\dfrac{< \xi^1 > \{\xi^2\} + < \xi^0 > \{\xi^3\}}{\|\{\xi^0\}\|_2^2}\right) \\ \quad + 2\left(< \gamma^1 > \{\gamma^2\} + < \gamma^0 > \{\gamma^3\}\right) \\ G = \dfrac{\|\{\gamma^0\}\|_2^2 C + E + D}{\|\{\gamma^0\}\|_2^2} \\ H = \dfrac{2 < \gamma^0 > \{\gamma^1\} C - 2\dfrac{< \xi^0 > \{\xi^1\}}{\|\{\xi^0\}\|_2^2} E + F}{\|\{\gamma^0\}\|_2^2} \end{cases} \tag{32}$$

As $E_M(a) = \varepsilon_p$, then

$$a^{M-1}\left(e_0 + e_1 a + e_2 a^2 + e_3 a^3 + O(a^4)\right) = \varepsilon_p \tag{33}$$

we deduce

$$a\left(e_0 + e_1 a + e_2 a^2 + e_3 a^3 + O(a^4)\right)^{\frac{1}{M-1}} - \varepsilon_p^{\frac{1}{M-1}} = 0 \tag{34}$$

which gives, after development truncated at the order 3 with respect to the parameter a, the following equality

$$A_3 a^3 + A_2 a^2 + a - A_1 + O(a^4) = 0 \tag{35}$$

where A_1, A_2, and A_3 are given by:

$$\begin{cases} A_1 = \left(\varepsilon_p^2 \dfrac{\|\{\xi^0\}\|_2^2}{\|\{\gamma^0\}\|_2^2}\right)^{\frac{1}{2M-2}} \\ A_2 = \dfrac{B}{2M-2} \\ A_3 = \dfrac{1}{2M-2}\left(\dfrac{\|\{\gamma^0\}\|_2^2 C + E + D}{\|\{\gamma^0\}\|_2^2}\right) + \dfrac{3-2M}{8(M-1)^2} B \end{cases} \tag{36}$$

By neglecting in (35) the term $O(a^4)$, we get the following equation:

$$A_3 a^3 + A_2 a^2 + a - A_1 = 0 \tag{37}$$

which is written as:

$$P(a) = a^3 + \beta_2 a^2 + \beta_1 a + \beta_0 = 0 \tag{38}$$

where β_0, β_1, and β_2 are given by:

$$\begin{cases} \beta_0 &= -\dfrac{A_1}{A_3} \\ \beta_1 &= \dfrac{1}{A_3} \\ \beta_2 &= \dfrac{A_2}{A_3} \end{cases} \tag{39}$$

References

[1] E. Riks, An incremental approach to the solution of snapping and buckling problems, Int. J. Solids Struct. 15 (7) (1979) 529–551.
[2] M.A. Crisfield, A fast incremental/iterative solution procedure that handles “snap-through”, in: Computational Methods in Nonlinear Structural and Solid Mechanics, Elsevier, 1981, pp. 55–62.
[3] A. Eriksson, Derivatives of tangential stiffness matrices for equilibrium path descriptions, Int. J. Numer. Methods Eng. 32 (5) (1991) 1093–1113.
[4] B.A. Memon, et al., Arc-length technique for nonlinear finite element analysis, J. Zhejiang Univ. Sci. A 5 (5) (2004) 618–628.
[5] G.J. Turvey, Y. Zhang, A computational and experimental analysis of the buckling, postbuckling and initial failure of pultruded GRP columns, Comput. Struct. 84 (22–23) (2006) 1527–1537.
[6] H. Saffari, I. Mansouri, Non-linear analysis of structures using two-point method, Int. J. Non-Linear Mech. 46 (6) (2011) 834–840.
[7] K. Liang, M. Ruess, M. Abdalla, Co-rotational finite element formulation used in the Koiter–Newton method for nonlinear buckling analyses, Finite Elem. Anal. Des. 116 (2016) 38–54.
[8] Y. Zhou, I. Stanciulescu, T. Eason, M. Spottswood, Nonlinear elastic buckling and postbuckling analysis of cylindrical panels, Finite Elem. Anal. Des. 96 (2015) 41–50.
[9] N. Damil, M. Potier-Ferry, A new method to compute perturbed bifurcations: application to the buckling of imperfect elastic structures, Int. J. Eng. Sci. 28 (9) (1990) 943–957.
[10] B. Cochelin, A path-following technique via an asymptotic-numerical method, Comput. Struct. 53 (5) (1994) 1181–1192.
[11] M. Potier-Ferry, N. Damil, B. Braikat, J. Descamps, J.-M. Cadou, H.L. Cao, A.E. Hussein, Traitement des fortes non-linéarités par la méthode asymptotique numérique, C. R. Acad. Sci. Paris, Sér. IIb 324 (3) (1997) 171–177.
[12] B. Braikat, N. Damil, M. Potier-Ferry, Méthodes asymptotiques numériques pour la plasticité, Rev. Eur. Éléments Finis 6 (3) (1997) 337–357.
[13] A. Elhage-Hussein, M. Potier-Ferry, N. Damil, A numerical continuation method based on Padé approximants, Int. J. Solids Struct. 37 (46–47) (2000) 6981–7001.
[14] M. Jamal, B. Braikat, S. Boutmir, N. Damil, M. Potier-Ferry, A high order implicit algorithm for solving instationary non-linear problems, Comput. Mech. 28 (5) (2002) 375–380.
[15] J.M. Cadou, N. Damil, M. Potier-Ferry, B. Braikat, Projection techniques to improve high-order iterative correctors, Finite Elem. Anal. Des. 41 (3) (2004) 285–309.
[16] B. Cochelin, N. Damil, M. Potier-Ferry, Méthode asymptotique numérique, Hermès Lavoisier, 2007.
[17] H. Mottaqui, B. Braikat, N. Damil, Local parameterization and the asymptotic numerical method, Math. Model. Nat. Phenom. 5 (7) (2010) 16–22.
[18] H. Mottaqui, B. Braikat, N. Damil, Discussion about parameterization in the asymptotic numerical method: application to nonlinear elastic shells, Comput. Methods Appl. Mech. Eng. 199 (25–28) (2010) 1701–1709.
[19] M.V. Dyke, Computer-extended series, Annu. Rev. Fluid Mech. 16 (1) (1984) 287–309.
[20] J. Van Iseghem, Vector Padé approximants, in: Numerical Mathematics and Applications, Elsevier, 1985, pp. 73–77.
[21] H. Padé, Sur la représentation approchée d'une fonction par des fractions rationnelles, vol. 740, Gauthier-Villars et fils, 1892.
[22] B. Cochelin, N. Damil, M. Potier-Ferry, Asymptotic–numerical methods and Padé approximants for non-linear elastic structures, Int. J. Numer. Methods Eng. 37 (7) (1994) 1187–1213.
[23] A. Hamdaoui, B. Braikat, N. Tounsi, N. Damil, On the use of Padé approximant in the Asymptotic Numerical Method ANM to compute the post-buckling of shells, Finite Elem. Anal. Des. 137 (2017) 1–10.
[24] J.L. Batoz, G. Dhatt, Modélisation des structures par éléments finis: Solides élastiques, Presses de l'université Laval, Québec, Canada, 1990.
[25] J.L. Batoz, G. Dhatt, Modélisation des structures par élément finis, vol. 3, Éditions Hermès, 1992.